Fluctuation potentials for intrashell electron pairs in some He and Belike systems

K. E. Banyard and J. Sanders

Citation: The Journal of Chemical Physics **94**, 6125 (1991); doi: 10.1063/1.460424
View online: http://dx.doi.org/10.1063/1.460424
View Table of Contents: http://scitation.aip.org/content/aip/journal/jcp/94/9?ver=pdfcov
Published by the AIP Publishing

Fluctuation potentials for intrashell electron pairs in some He- and Be-like systems

K. E. Banyard and J. Sanders
Department of Physics and Astronomy, University of Leicester, Leicester, England

(Received 26 June 1990; accepted 18 January 1991)

Electron correlation is determined by the deviation of the Coulombic repulsion potential from the Hartree–Fock average potential. This deviation is termed a fluctuation potential. Investigated here, for the first time, are the Z-dependent characteristics and the range of such fluctuation potentials for a series of He- and Be-like ions. Each system is in its ground state. Results for the separate intrashell electron pairs are presented as potential profiles and scaled contour diagrams. For these K and L shells, the radial and angular components of electron correlation—and their changes in relative importance with increasing Z—can be seen to arise from specific features in the associated fluctuation potentials. The extent of each potential difference is assessed with respect to a defined "range of shell" distance. Previously, fluctuation potentials had been presumed to be short ranged. The present work indicates that this is not the case.

I. INTRODUCTION

For several decades, considerable effort has been devoted to devising and obtaining approximate solutions[1–4] for the many-body Schrödinger equation which go beyond the Hartree–Fock (HF) method.[5] Being an independent-particle model, the HF treatment provides only an averaged account of the correlated motions of the particles. The resulting error in the total energy calculated for an atomic or a molecular problem, although small in percentage terms, is important when discussing the energy *variations* which occur in chemical reactions.[4,6] Further, for such systems an effective description of the correlated motions of the electrons will have a significant influence on the two-particle density distribution and, to a lesser extent, on the one-particle distribution. Correlation-induced density changes have been examined by several workers[7–12] and involve such concepts as the Coulomb hole,[13–16] intracule and extracule functions,[17] statistical correlation coefficients,[18] and, when working in momentum space, the Coulomb shift.[19] In each instance the changes are measured with respect to the corresponding HF results.

Clearly, electron correlation[20] is determined by the *deviation* of the instantaneous Coulomb potential between a pair of electrons from the average potential they exert on one another, as determined by the HF approach. This deviation is referred to as the *fluctuation potential*[21] and, since it is the difference between two relatively long-range effects, it is thought to be shortranged.[22] Its occurrence in the formal development of an energy calculation has been discussed extensively by Sinanoğlu and co-workers.[21–26] (See also the energy analysis by Hata[27] in which he considers the screening of a fluctuation potential by other HF particles.) Although all correlation effects arise directly from the existence of a fluctuation potential, it has not previously been appraised in any detail. Hence we examine here the characteristics of the potential, its range, relative importance, and, in particular, its Z-dependent trends. To simplify the investigation, and since the correlation energy is dominated by intrashell contributions,[28–31] our initial study of fluctuation potentials is restricted to the doubly occupied K and L shells within a series of He(^1S)-like and Be(^1S)-like ions, as appropriate. Such an examination complements earlier work[7,32–34] and parallels the increasing interest in the correlation problem.[35–45]

II. CALCULATION AND RESULTS

In the many-electron theory of Sinanoğlu,[24,28] it has been demonstrated how the energy of a system may be resolved into the HF contribution and the correlation part. The latter component involves the complete fluctuation potential m_{ij} which, being of operator form, makes any graphical presentation of such a quantity not strictly feasible (see Sinanoğlu[22,24,46] and, e.g., Parr[47] for further details of m_{ij}). Instead, for ease of interpretation, we follow Sinanoğlu[21,22] and examine the more physically intuitive[3,21,22,30,48] expression for a fluctuation potential given by

$$S(\mathbf{r}_1;\mathbf{r}_2)=\frac{1}{r_{12}}-\int \phi^*(\mathbf{x}_1)\frac{1}{r_{12}}\phi(\mathbf{x}_1)d\mathbf{x}_1. \qquad (1)$$

For the electron pair (1,2), $S(\mathbf{r}_1;\mathbf{r}_2)$ represents the difference between the instantaneous repulsion term r_{12}^{-1} and the average HF potential V_{HF}. From a labeling point of view, the first term may be regarded as the potential experienced by the "roving" or moving electron 2 due to electron 1 being placed at some *fixed* position relative to the origin; the second term is the average potential, evaluated at the location of the moving electron 2, when electron 1 is described by the HF spin–orbital $\phi(\mathbf{x}_1)$, where $\mathbf{x}_1$ is the combined space–spin coordinate of electron 1. Atomic units are used throughout this work and all distances are measured from the nucleus as the origin of coordinates. The $S(\mathbf{r}_1;\mathbf{r}_2)$ function is examined for the electron pairs (1,2) within the K shells of H^-, He, Li^+, and Be^{++} and, similarly, for the separate K and L shells within Li^-, Be, B^+, C^{++}, N^{+3}, and O^{+4}. In each instance we used the ground state HF orbitals produced by Clementi and Roetti.[49] The energetically best functions reported by them yielded, via the integral in Eq. (1), a more than sufficiently accurate HF potential for the present work.

 0021-9606/91/096125-07$03.00

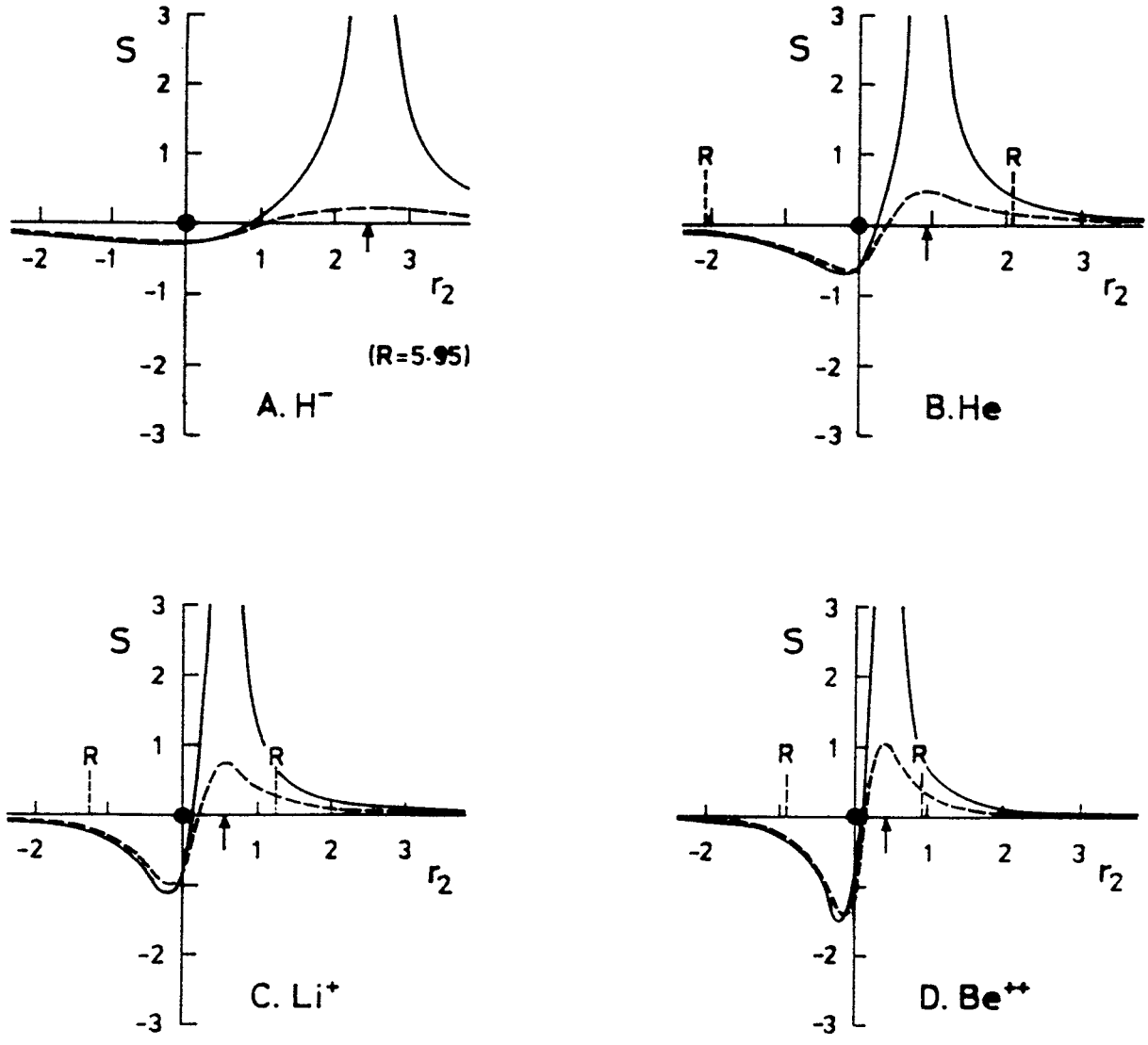

FIG. 1. The K-shell fluctuation potential $S = S(\mathbf{r}_1,\mathbf{r}_2)$ for (A)H$^-$, (B)He, (C)Li$^+$, and (D)Be^{++} when the fixed or test electron 1 is located at the Hartree–Fock (HF) expectation value $\langle r_1\rangle_{1s}$. The $\langle r_1\rangle_{1s}$ value is indicated by the arrow along the positive r_2 axis. The solid and dashed curves represent, respectively, profiles of $S(\mathbf{r}_1;\mathbf{r})$ evaluated along the nucleus-fixed electron axis and along a line at 45° to it, which also passes through the nuclear origin. R is the range of shell value. Throughout this work, atomic units are used and, in addition, the negative sign along the r_2 axis merely indicates a distance behind the nucleus, i.e., on the opposite side to the fixed electron.

For the K shells of the two-electron systems, fluctuation potentials are presented in Fig. 1 when electron 1 is fixed at $r_1 = \langle r_1\rangle_{1s}$, the 1$s$ expectation value. The solid curves indicate the $S(\mathbf{r}_1;\mathbf{r}_2)$ profiles plotted along a line joining the nucleus to the *fixed* electron position; the dashed curves represent the fluctuation potential evaluated along a line passing through the origin but at 45° to the "nucleus-fixed electron" line. Similar sets of profiles are shown in Fig. 2 for the L shells in Li$^-$, Be, B$^+$, and C^{++} when the fixed electron is located at $r_1 = \langle r_1\rangle_{2s}$. Profile diagrams are ideally suited for visualizing the overlap between the K and L-shell fluctuation potentials. Hence, for the examples of Be and N^{+3}, a measure of the overlap is provided in Figs. 3(A) and 3(B), respectively, by plotting the K- and L-shell results for each system on a common scale. Included in these diagrams, for discussion purposes, are the HF potentials for the individual shells. We note that each $V_{\rm HF}$, derived from the integral expression in Eq. (1), is spherically symmetric about the nucleus. The *relative* importance of a fluctuation potential enables us to examine the overlap from a different aspect. Thus the $S(\mathbf{r}_1;\mathbf{r}_2)$ function for a given shell is expressed as a percentage of the appropriate $V_{\rm HF}$ values. These K- and L-shell percentages are shown in Fig. 3(C) for Be and Fig. 3(D) for N^{+3}. The results for each diagram in Fig. 3 correspond to variations along the nucleus-fixed electron line only. A more general view of the K- and L-shell results for the Be-like ions is given in Fig. 4 where *contour* diagrams of the fluctuation potentials are shown for selected Z. The test electron is located at the expectation value in each instance. For the purposes of comparison, each diagram has been scaled such that the radius of its perimeter equals R, the range of shell distance. This qualitative measure R is defined

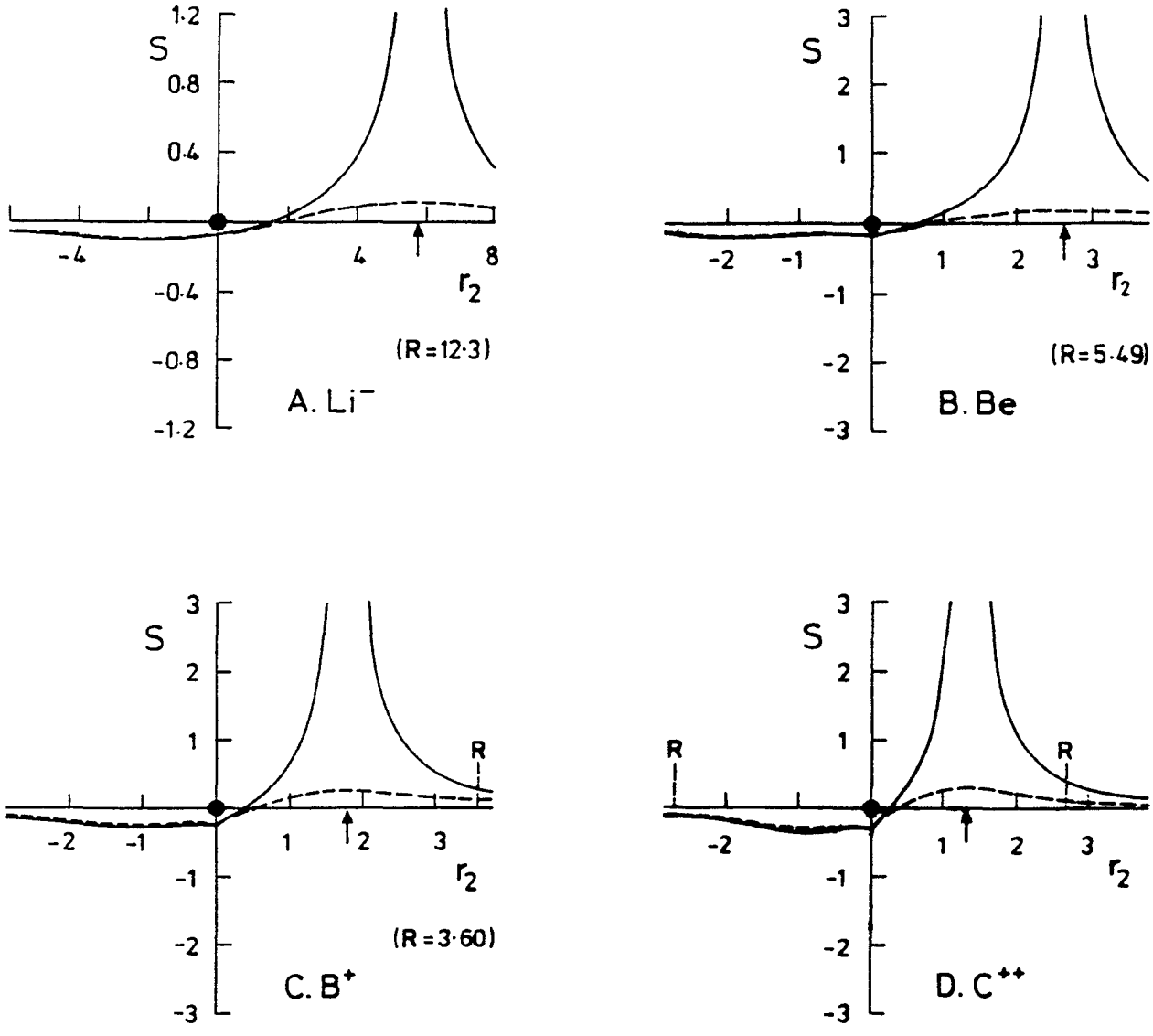

FIG. 2. The L-shell fluctuation potential $S(\mathbf{r}_1;\mathbf{r}_2)$ for the $(2s)^2$ electron pair in (A) Li^-, (B) Be, (C) B^+, and (D) C^{++} when the fixed electron 1 is located at the HF expectation value $\langle r_1\rangle_{2s}$. The $\langle r_1\rangle_{2s}$ value is indicated by the arrow along the positive r_2 axis. The solid and dashed curves represent the $S(\mathbf{r}_1;\mathbf{r}_2)$ profiles evaluated as before. R is the range of shell value. Note the different scales for diagram (A).

as the radius of a sphere, centered on the nucleus, which encompasses 95% of the HF charge distribution for that shell.

In Table I, we report the HF expectation values $\langle r_1\rangle_{1s}$ and $\langle r_1\rangle_{2s}$ for the individual K and L shells examined here. Included in Table I are the range of shell distances R, as defined above.

III. DISCUSSION

The relative extent of the $S(\mathbf{r}_1;\mathbf{r}_2)$ profiles shown in Figs. 1, 2, and 3 may be judged by comparison with the R values given in each instance. When $r_1 = \langle r_1\rangle_{1s}$ for the K shells, Fig. 1 indicates that the fluctuation potential for H^- is essentially confined within a sphere of radius R. By contrast, the Be^{++} results are seen to be of sizable magnitude when $|r_2| = R$. As expected, the $S(\mathbf{r}_1;\mathbf{r}_2)$ function rises to infinity when the roving electron approaches the "fixed" or "test" electron. Further, as Z gets larger, we observe that the range of the negative region in $S(\mathbf{r}_1;\mathbf{r}_2)$ becomes less extensive in absolute terms and its depth increases significantly. When an allowance is made for electron correlation, a region of negative fluctuation potential will, of course, result in a local *increase* in the electron probability density. Consequently, the general extent of such a region ought to be located "behind" the nucleus, i.e., on the opposite side to the fixed electron. This is confirmed in Fig. 1.

The exact interelectronic potential r_{12}^{-1} in Eq. (1) corresponds to total correlation between the two electrons and could, in principle, be described by, for example, an elaborate Hylleraas-type wave function. Since the correlation effect within an atomic wave function can be analyzed in terms of its "radial" and "angular" components, it is reasonable to examine $S(\mathbf{r}_1;\mathbf{r}_2)$ for the associated characteristics. For H^-, the "in line" and 45° profiles in Fig. 1(A) show that the slowly varying negative region of $S(\mathbf{r}_1;\mathbf{r}_2)$ extends consider-

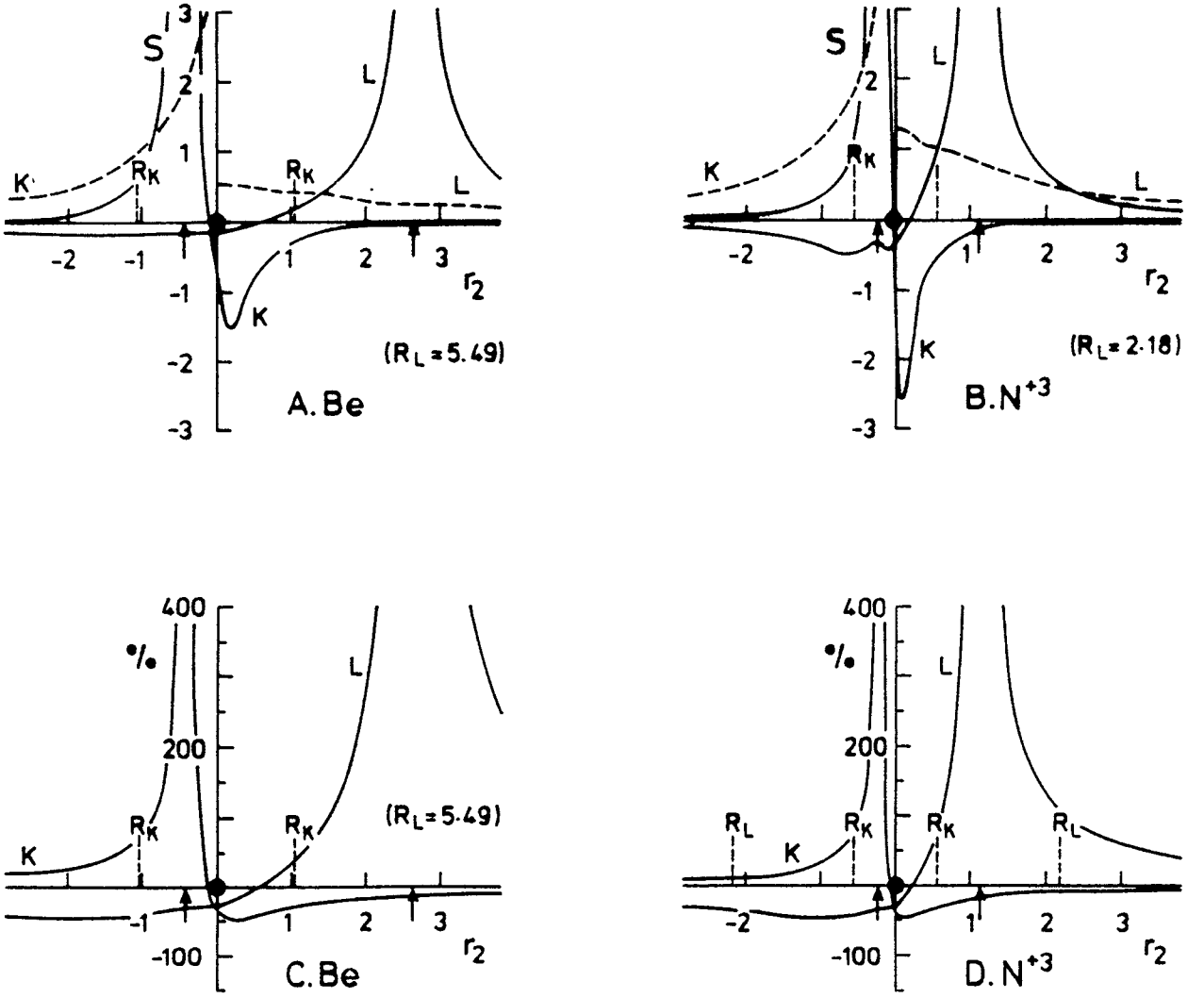

FIG. 3. A comparison between the $S(\mathbf{r}_1;\mathbf{r}_2)$ profiles for the individual K and L shells within the four-electron systems (A)Be and (B)N^{+3}; see the solid curves. The dashed curves in (A) and (B) represent the spherically symmetric potentials V_{HF} where, for clarity, the K- and L-shell results are shown only on the left and right, respectively, of each nuclear origin. In (C)Be and (D) N^{+3}, a comparison between the K and L shells is made of the *relative* importance of each profile, expressed as a *percentage* of the appropriate V_{HF} value. Throughout (A)–(D), the fixed electrons for the K and L shells are located (as shown by the arrows) on the left and right of the nucleus, respectively, at distances equal to the corresponding $\langle r_1 \rangle$. R_K and R_L indicate the separate K and L range of shell distances (see Table I).

ably *towards* the location of the test electron. In addition, the shallow minimum is seen to be in close proximity to the nucleus. However, for Be^{++}, the negative region of the profiles is markedly less extensive in "front" of the nucleus, it is also more rapidly varying, and its well-defined minimum is clearly located further behind the nucleus. Indeed, although the contour diagrams in Fig. 4 relate to Be-like systems, these changes in K-shell characteristics still occur, as expected, and become even more apparent when $Z = 8$. As seen, the relative distance of the minimum behind the nucleus for $Z = 8$ is over 50% greater than that found for $Z = 4$. Such observations are in accord with the reported[7,11] dominance of radial correlation for H^- and, in particular, the steady change in location of the K-shell minimum is in keeping with the known[7,18] increase in relative importance of angular correlation, as Z gets larger.

The above interpretation of a fluctuation potential is supported by examining its behavior, for the example of He, when the fixed electron is located at different r_1 values. Although not shown here for reasons of space, placing the test electron on the He nucleus produced a spherically symmetric $S(\mathbf{r}_1;\mathbf{r}_2)$ function which was everywhere *positive*. Thus as might be expected, the correlation effect would be totally radial in nature and would shift probability density, associated with the roving electron, away from the nucleus. As the fixed electron was moved off the origin, a shallow minimum developed in the fluctuation potential far behind the nucleus. A progressive increase in the fixed r_1 value caused the minimum to increase in depth *and* to approach the nucleus. Since the roving electron will tend to seek a potential minimum, this behavior of the fluctuation potential reveals the presence of *angular* correlation and indicates the nature of its variation. When r_1 exceeds $2\langle r_1 \rangle_{1s}$, the minimum was found to be coincident with the He nucleus which, in turn, is sur-

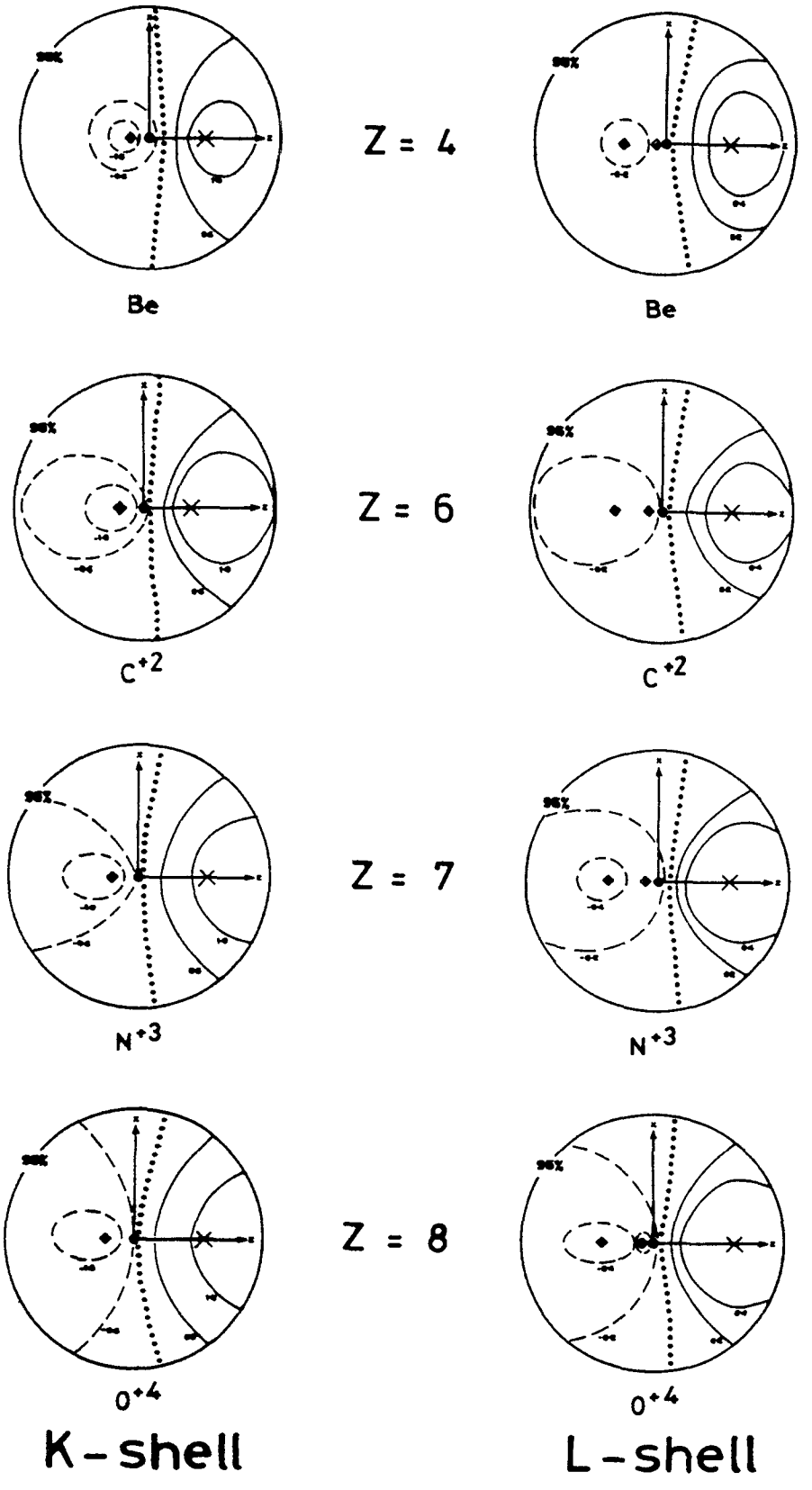

FIG. 4. Contour diagrams of $S(\mathbf{r}_1;\mathbf{r}_2)$ for the K and L shells within the four-electron systems Be, C^{+2}, N^{+3}, and O^{+4}. The K-shell diagrams are in the left-hand column and the L-shell results are on the right. Z is the nuclear charge. For each shell, the fixed electron 1 is located at X on the arbitrary horizontal z axis, the distance from the origin (the nucleus) being, as before, equal to $\langle r_1 \rangle$; see Table I. In each contour diagram, the minimum is marked by $\diamondsuit$ and the negative, zero, and positive contours are indicated by dashed, dotted, and solid lines, respectively. Taken in order from the maximum (at X) to the minimum (at $\diamondsuit$), the K-shell contours range from $+1.0$, (-0.5), -1.0. The L-shell contours are similarly ordered in the range $+0.4$, (-0.2), -0.2 for $Z=4$ and 6, and down to -0.4 for $Z=7$ and 8. The 95% boundary has a radius equal to R: the range of shell value. For comparison, each R has been scaled to a common physical size.

rounded by a sizable region of *negative* $S(\mathbf{r}_1;\mathbf{r}_2)$ values. Although this negative region had a boundary which was asymmetric in shape about the origin (thus confirming the continued existence of an angular effect), its essential characteristics are compatible with a localized region dominated by radial correlation. In this instance, the radial effect would result in an *increase* in the probability density of the roving electron being found around the nucleus.

The fluctuation potential $S(\mathbf{r}_1;\mathbf{r}_2)$ for the L-shell $(2s)^2$ electron pair in the four-electron systems (see Fig. 2) shows

TABLE I. Hartree–Fock expectation values $\langle r_1 \rangle$ and the range of shell values R, for the He(^1S)-like K shells and the Be(^1S)-like K and L shells for various values of Z, the nuclear charge. Atomic units are used.

	He-like		Be-like			
	$K(1s)^2$		$K(1s)^2$		$L(2s)^2$	
Z	$\langle r_1 \rangle$	R	$\langle r_1 \rangle$	R	$\langle r_1 \rangle$	R
1	2.466	5.951	...	...	...	...
2	0.927	2.082	...	...	...	...
3	0.572	1.238	0.573	1.255	5.748	12.32
4	0.414	0.898	0.415	1.028	2.649	5.488
5	0.324	0.698	0.325	0.805	1.798	3.598
6	...	...	0.267	0.665	1.372	2.705
7	...	...	0.227	0.568	1.112	2.175
8	...	...	0.197	0.472	0.936	1.582

several points of contrast with the K-shell results. When viewed collectively, the L-shell curves are found to be much shallower, and more slowly varying, in their negative regions than the K-shell profiles. More specifically, it is noted that the Li^- profiles in Fig. 2(A) have different scales from the rest of the series. The L-shell results generally are seen to possess a double minima; this feature is associated with the double maxima which occurs in the HF 2s-orbital probability density. Further, we observe that the principal minimum in each $S(\mathbf{r}_1;\mathbf{r}_2)$ function is located well behind the nucleus.

The Z variations of the L-shell profiles in Fig. 2 are somewhat less obvious than those for the K shell in Fig. 1. However, for Li^-, the negative region of $S(\mathbf{r}_1;\mathbf{r}_2)$ is seen to extend considerably in front of the nucleus, being about 50% further than that observed for the K-shell negative ion H^-. Thus, when the $(2s)^2$ electron pair is described by a correlated wave function, this feature indicates that a localized region of radial correlation will occur around the Li nucleus, along with a consequent increase in probability density. Although the negative region in Fig. 2(A) for Li^- is quite shallow, the location of the principal minima away from the nucleus denotes the presence of an angular component of correlation. When Z is increased, the L-shell profiles show a curtailment of the radial effect around the origin and a slight but definite emphasis of the relative angular effect behind each nucleus.

When presenting the K- and L-shell fluctuation potentials on a common scale, the two fixed electrons were located on opposite sides of the nucleus; the distances being, as before, $\langle r_1 \rangle_{1s}$ and $\langle r_1 \rangle_{2s}$. Comparisons between the corresponding profiles for the examples of Be and N^{+3} are shown in Figs. 3(A) and 3(B), respectively. To place the test electrons on the *same* side of the nucleus would have exaggerated the overlap between the two $S(\mathbf{r}_1;\mathbf{r}_2)$ functions. An alternative presentation which gives a different view of the overlap, but is pictorially more cumbersome, would have been to arrange the nucleus-fixed electron line for the K shell at 90° to that for the L shell.

For the fixed electron positions used in Fig. 3(A), the individual 1s and 2s profiles for Be show a clear separation between the respective maxima. The major region of overlap appears to be confined within the vicinity of the origin where the K-shell effect is obviously dominant. This would also hold true if, as mentioned above, the $S(\mathbf{r}_1;\mathbf{r}_2)$ functions were orientated at 90°. For the corresponding locations of the fixed electrons in N^{+3}, Fig. 3(B) shows similar features. However, the fluctuation potential for the L shell would now make a more significant contribution to the sum *total* effect around the nucleus. In each diagram, the combined effect of the K- and L-shell profiles would tend to emphasize the separation of the two maxima by reducing the positive values in the region between the two infinite peaks. Such partial cancellations of these separate K- and L-shell fluctuation potentials will, of course, occur for many other locations of the test electrons. However, if the test electrons were in close proximity (and on the same side of the nucleus) then, naturally, the combined effect between the two peaks could remain positive and increase in magnitude.

When comparing the *relative* importance of the individual intrashell fluctuation potentials within Be and N^{+3} [see Figs. 3(C) and 3(D)], it will be useful to refer to the V_{HF} curves shown in Figs. 3(A) and 3(B). We note that all four diagrams have the same arrangement for the fixed electrons. Figure 3(C) indicates that the percentage profiles, relating the $S(\mathbf{r}_1;\mathbf{r}_2)$ results to the corresponding V_{HF} values, have negative regions for the Be K and L shells which are of comparable magnitude. Such comparability is even more apparent in Fig. 3(D) for N^{+3}. This is in clear contrast with the behavior of the negative values for the K- and L- shell fluctuation potentials shown in Figs. 3(A) and 3(B). Further, the relative importance of the L-shell fluctuation potential is seen to vary between -40% and $+40\%$ over the marked *K-shell* range R for Be, and between -40% and $+80\%$ over the *K-shell* range for N^{+3}. The respective sizes of the HF potentials for the individual K and L shells, evaluated over the range of the corresponding K shell, can be judged by inspection of Fig. 3(A) or 3(B), as appropriate; we recall that each V_{HF} is, of course, spherically symmetric.

The percentage profile for each shell, shown in Fig. 3, remains sizable even beyond the range of shell value. For the L shell in Be, the percentages at the range of shell distance R are about -30% and $+120\%$. From a percentage viewpoint, these K- and L-shell fluctuation potentials are found to have a more extensive range than was originally anticipated. However, it is obvious that, by comparison with percentages near the fixed electron, such effects are small.

In Fig. 4 we see that the contour diagrams of the K-shell fluctuation potentials support our earlier observations. Not only does an increase in Z produce a deeper and more extensive negative region behind the nucleus but, with respect to R, the minimum is seen to be located progressively further away from the nucleus. Of particular note is the change in curvature of the zero contour (when V_{HF} equals the exact potential) for the K shell as we progress from Be to O^{+4}. In addition, the positive region becomes more pronounced and, like the negative region, extends well beyond the range of shell boundary when $Z = 8$.

For the L shells, the contours in Fig. 4 show that, as Z becomes larger, an increase occurs in magnitude and extent for the negative and positive regions. The curvature of the zero contour is seen to be more slowly varying than that for

the K shell. For each $Z \geqslant 6$, we observe that the zero contours for the K and L shells cross the nucleus-fixed electron line in front of the nucleus at distances which, with respect to the appropriate R value, are roughly comparable. However, a significant point of contrast between the K- and L-shell contour plots is that, for each L shell, the principal minimum is *always* located well behind the nucleus: the scaled distance being noticeably in excess of that for the corresponding K shell. Thus, for a Be-like ion, these features of the fluctuation potential mean that the angular component of correlation will be relatively more important in the L shell than in the K shell.

IV. SUMMARY

The fluctuation potential for an electron pair is the difference between the interparticle Coulombic repulsion potential and the Hartree–Fock average effect. As such, its existence is the basic cause of all correlation effects. Examined here, for the first time, are fluctuation potentials for the separate intrashells within the He- and Be-like series of ions. Consequently, we have been able to consider how the characteristics, range and Z-dependent variations of these potentials influence the relative importance of the radial and angular components of correlation for the $(1s)^2$ and $(2s)^2$ electron pairs.

For the He-like systems, the fluctuation potential $S(\mathbf{r}_1;\mathbf{r}_2)$ for $Z = 1$ could be interpreted as being consistent with a preponderance of the *radial* component of electron correlation. When Z was increased, the progressive movement of the minimum in $S(\mathbf{r}_1;\mathbf{r}_2)$ away from the nucleus revealed a growth in the relative importance of the *angular* component of K-shell correlation. Contour diagrams for the Be-like L-shell potentials had characteristics which, by comparison with the K shells,indicated that angular correlation was *always* relatively more significant in the L shell than for the K shell.

When considering the overlap between the K- and L-shell fluctuation potentials for the Be-like systems, the two infinite peaks obviously preserved a distinctness between them. Nevertheless, some considerable overlap between the two intrashell $S(\mathbf{r}_1;\mathbf{r}_2)$ functions did exist over the range of the appropriate K shell. Further, in the past, it has been presumed that a fluctuation potential, being the difference between two relatively long range potentials, was itself *short* ranged. The present investigation suggests that this is not the case.

Finally, although this initial work was confined to atomic ions, it is felt that, before performing any lengthy calculation which involves electron correlation, a brief examination of the fluctuation potential could be informative.

ACKNOWLEDGMENT

One of us, J. S., wishes to express gratitude for an S.E.R.C. research grant.

[1] C. L. Pekeris, Phys. Rev. **115**, 1216 (1959).
[2] S. F. Boys and N. C. Handy, Proc. R. Soc. London Ser. A **309**, 209 (1969).
[3] K. Jankowski, in *Methods in Computational Chemistry, Vol. 1, Electron Correlation in Atoms and Molecules*, edited by S. Wilson (Plenum, New York, 1987), p. 1.
[4] M. Urban, I. Černušák, V. Kellö, and J. Noca, in *Methods in Computational Chemistry*, edited by S. Wilson (Plenum, New York, 1987), Vol. 1, p. 117.
[5] C. Froese Fischer, *The Hartree–Fock Method for Atoms* (Wiley, New York, 1977).
[6] H. F. Schaeffer III, Science **231**, 1100 (1986).
[7] K. E. Banyard and C. C. Baker, J. Chem. Phys. **51**, 2680 (1969).
[8] R. Benesch and V. H. Smith, Jr., Int. J. Quantum Chem. **S4**, 131 (1971).
[9] K. E. Banyard, An. Fis. **67**, 409 (1971).
[10] V. H. Smith, Jr. and R. E. Brown, Chem. Phys. Lett. **20**, 424 (1973).
[11] R. J. Boyd, Chem. Phys. Lett. **44**, 363 (1976).
[12] A. Gupta and R. J. Boyd, J. Chem. Phys. **68**, 1951 (1978).
[13] C. A. Coulson and A. H. Neilson, Phys. Soc. (London) **78**, 831 (1961).
[14] K. E. Banyard and D. J. Ellis, Mol. Phys. **24**, 1291 (1972).
[15] R. J. Boyd and C. A. Coulson, J. Phys. B **6**, 782 (1973).
[16] G. Doggett, Mol. Phys. **38**, 853 (1979).
[17] A. J. Thakkar, in *Density Matrices and Density Functionals*, edited by R. M. Erdahl and V. H. Smith, Jr. (Dordrecht, Reidel, 1987), p. 553.
[18] W. Kutzelnigg, G. Del Re, and G. Berthier, Phys. Rev. **172**, 49 (1968). See also, A. J. Thakkar and V. H. Smith, Jr., Phys. Rev. A **23**, 473 (1981).
[19] K. E. Banyard, K. H. Al-Bayati, and P. K. Youngman, J. Phys. B **21**, 3177 (1988); see also, Corrigendum: *ibid.* **22**, 971 (1989).
[20] P. L. Löwdin, Adv. Chem. Phys. **2**, 207 (1959).
[21] O. Sinanoğlu, Proc. Natl. Acad. Sci. U.S.A. **47**, 1217 (1961).
[22] O. Sinanoğlu, J. Chem. Phys. **36**, 706, 3198 (1962).
[23] O. Sinanoğlu and D. F. Tuan, J. Chem. Phys. **38**, 1740 (1963).
[24] O. Sinanoğlu, Adv. Chem. Phys. **6**, 315 (1964).
[25] V. McKoy and O. Sinanoğlu, J. Chem. Phys. **41**, 2689 (1964).
[26] H. J. Silverstone and O. Sinanoğlu, J. Chem. Phys. **44**, 1899, 3608 (1966).
[27] J. Hata, Chem. Phys. Lett. **24**, 373 (1974).
[28] O. Sinanoğlu and K. A. Brueckner, *Three Approaches to Electron Correlation in Atoms* (Yale, New Haven, 1970).
[29] B. Roos, in *Computational Techniques in Quantum Chemistry and Molecular Physics*, edited by G. H.F. Diercksen, B.T. Sutcliffe, and A. Veillard (Reidel, Dordrecht, 1975), p. 251.
[30] W. Kutzelnigg, in *Methods of Electronic Structure Theory*, edited by H. S. Schaefer III (Plenum, New York, 1977), p. 129.
[31] S. Wilson, *Electron Correlation in Molecules* (Clarendon, Oxford, 1984).
[32] R. Benesch and V. H. Smith, Jr., J. Chem. Phys. **55**, 482 (1971).
[33] K. E. Banyard and M. M. Mashat, J. Chem. Phys. **67**, 1405 (1977).
[34] K. E. Banyard and R. J. Mobbs, J. Chem. Phys. **75**, 3433 (1981).
[35] Lui Tong-jiang, Zhang Zhi-jie, and Zhao Yi-jun, J. Phys. B **21**, 535 (1988).
[36] S. Wilson, *The Many-body Perturbation Theory of Atoms and Molecules* (Hilger, Bristol, 1988).
[37] S. Fraga, E. San Fabian, J. A. Sordo, M. Campillo, J. D. Climenhaga, and M. Klobukowski, Int. J. Quantum Chem. **35**, 325 (1989).
[38] N. C. Handy, J. A. Pople, M. Head-Gordon, K. Raghavachari, and G. W. Trucks, Chem. Phys. Lett. **164**, 185 (1989).
[39] P. Fuentealba, A. Savin, H. Stoll, and H. Preuss, Phys. Rev. A **41**, 1238 (1990).
[40] D. Frye, A. Preiskorn, G. C. Lie, and E. Clementi, J. Chem. Phys. **92**, 4948 (1990).
[41] L. A. Curtiss, C. Jones, G. W. Trucks, K. Raghavachari, and J. A. Pople, J. Chem. Phys. **93**, 2537 (1990).
[42] F. W. King and M. P. Bergsbaken, J. Chem. Phys. **93**, 2570 (1990).
[43] G. B. Armen, B. I. Craig, F. P. Larkins, and J. A. Richards, J. Electron Spectrosc. Relat. Phenom. **51**, 183 (1990).
[44] P. Dutta and S. P. Bhattacharyya, Phys. Lett. A **148**, 331 (1990).
[45] C-M. Liekgener, A. Sutjianto, and J. Ladik, Chem. Phys. **145**, 385 (1990).
[46] O. Sinanoğlu, Adv. Chem. Phys. **14**, 237 (1969).
[47] R. G. Parr, *Quantum Theory of Molecular Electronic Structure* (Benjamin, New York, 1964), p. 116.
[48] H. P. Kelly, Phys. Rev. **114**, 39 (1966).
[49] E. Clementi and C. Roetti, At. Data Nucl. Data Tables **114**, 177 (1974).